A VIRTUAL PISTON-TYPE WAVE MAKER BASED ON OPENFOAM

(DOI No: 10.3940/rina.ijme.2017.a2.407)

J Yao, Key Laboratory of High Performance Ship Technology (Wuhan University of Technology), Ministry of Education, Wuhan, P. R. China; School of Transportation, Wuhan University of Technology, Wuhan, P. R. China.

SUMMARY

OpenFOAM is an open source CFD (Computational Fluid Dynamics) toolbox and recently attracts many researchers to develop codes based on it for their own applications. In order to numerically generate waves based on the wave-maker theory for a piston motion, numerical improvements have been done on the base of OpenFOAM by the author. In general, the present new tool can be employed to simulate wave generation as long as the piston motion is given. This paper presents the related computational procedure and simulations for generating relatively long finite-amplitude waves according to Madsen's second-order wave-maker theory. The sensitivities of the computed incident wave profile to grid density and time step are investigated for the case of generating a wave with permanent form. The simulation accuracy is validated by comparison with the analytical solution and available experimental data.

1. INTRODUCTION

Havelock (1929) is most probably the first researcher who carried out the studies on wave-maker theory. He derived analytical solutions of linear wave generations for piston- and flap-type wave maker. Ursell et al. (1960) did an experimental study to verify the linear wave-maker theory for a piston motion. In 1970s, the second-order wave-maker theory received amount of attentions. It is generally recognized that if the displacement of a piston is prescribed to be sinusoidal, the resulting finite-amplitude wave will consist of a primary and one or more secondary waves, not showing a permanent form. The frequency of primary wave will be the same with that of the wave maker, however, the frequencies of the secondary waves differ from that. Thereafter, Madsen (1971) came up with a theory of second-order wave maker. He expounded the components of the resulting wave induced by the sinusoidal motion of a piston, and gave out their mathematic formulas of wave profile derived from potential theory. In particular, he discovered a wave-maker motion which eliminates the secondary harmonic free wave, consequently resulting in that the generated wave was absolutely progressive and of permanent form. Sulisz and Hudspeth (1993) developed a complete second-order solution for a generic wave maker. Later on, the studies on the theory of nonlinear wave generations were more reported in publications. For example, Schäffer (1996) proposed a wave-maker theory for irregular waves. The theory was demonstrated for a piston-type wave maker in laboratory. Zhang and Schäffer (2007) did an experimental study on verifying their approximate stream function wave-maker theory for highly non-linear waves. More recently, Sulisz and Praprota (2008) performed a prediction study on the propagation and transformation of non-linear water waves.

As the development of wave-maker theory, more natural waves can be generated in wave tank now. This is of significance for the studies on hydrodynamic performance of offshore structures in waves. In the initial stage of design for a marine structure, we can obtain its dynamic response in its working environment simulated in a wave tank, and finally guide the design for safety. To date, most wave makers equipped in wave tank are either piston- or flap-type. How to artificially reproduce natural waves in laboratory remains a big challenge as yet.

The concept of "numerical wave tank" has appeared in past decades. Wave generations can be numerically simulated by means of CFD methods and this concept is being increasingly used as an alternative to real wave tanks. Its evident advantages are that CFD technique reduces the period and cost of research, e.g., the study on ship seakeeping performance, and meanwhile offers more flow details which is helpful for better understanding about related mechanisms. So far there are two main numerical approaches for simulating wave generations: one assumes the fluids to be inviscid and non-rotational, i.e. the so-called potential theory; the other deals with the viscous fluids. In the former approach, the Laplace equation together with boundary conditions is solved, usually using a boundary element method (Grilli et al., 2001), while in the latter method the governing equations are Navier-Stokes (NS) (Dong and Huang, 2001) or Reynolds-Averaged Navier-Stokes (RANS) equations. In recent years, the latter method seems to be more preferable as reflected in literatures. Part of the reason may be that in many applications viscosity affects much the simulation accuracy and thus is non-ignorable. Another way to generate wave via NS or RANS simulations is to set internal flow velocity at an inlet boundary of the computational domain (Hafsia et al., 2009). The velocity on inlet must be prescribed according to the desired wave profile. This method for wave generation shows its advantages on computational efficiency in practical applications since it avoids the dynamic mesh involved in the simulations of physical wave maker.

The author has developed an own dynamic boundary condition and a solver for simulations of piston-type wave maker based on OpenFOAM. This study will focus on the verification and validation of the accuracy of the generated wave profiles. The cases of two dimensions are considered in the simulations according to the Madsen's

©2017: The Royal Institution of Naval Architects

second-order wave-maker theory. The computed wave profiles are compared with experimental data and analytical solutions.

2. GOVERNING EQUATIONS AND INITIAL AND BOUNDARY CONDITIONS

In this study, the generations of 2D waves are simulated. Figure 1 displays the sketch of a piston-type wave maker. In the figure, h denotes the still water depth, x-axis is horizontal and locates in still water surface, z-axis is vertical upwards and locates at the initial position of the piston. The piston moves periodically along the x-axis and its displacement ξ is prescribed in advance for a desired wave according to a certain theory of wave generation.

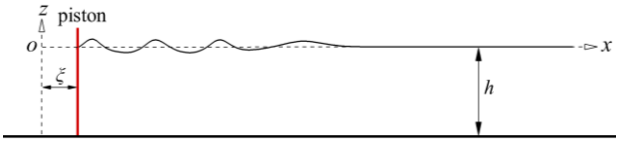

Figure 1 Sketch of a piston-type wave maker and coordinate system

In order to simulate the physical wave maker, the unsteady NS equations are solved. For incompressible fluids, the continuity equation in above Cartesian coordinate system is

$$\frac{\partial u}{\partial x}+\frac{\partial w}{\partial z}=0 \tag{1}$$

and the NS equations are

$$\begin{aligned}\frac{\partial u}{\partial t}+u\frac{\partial u}{\partial x}+w\frac{\partial u}{\partial z}&\\ =-\frac{1}{\rho}\frac{\partial p}{\partial x}&\\ +\nu\left(\frac{\partial^2 u}{\partial x^2}+\frac{\partial^2 u}{\partial z^2}\right)&\\ -d(x)u&\end{aligned} \tag{2}$$

$$\begin{aligned}\frac{\partial w}{\partial t}+u\frac{\partial w}{\partial x}+w\frac{\partial w}{\partial z}&\\ =-g-\frac{1}{\rho}\frac{\partial p}{\partial z}+\nu\left(\frac{\partial^2 w}{\partial x^2}+\frac{\partial^2 w}{\partial z^2}\right)&\\ -d(x)w&\end{aligned} \tag{3}$$

where u and w are velocity components, ν is kinematic viscosity, p is pressure, ρ is density of fluid, t is time, g is gravitational acceleration and $d(x)$ is a damping function which is equal to zero except for the dissipation zone located in the end part of the virtual wave tank. Here a linear damping law is assumed to be as

$$d(x)=\alpha(x-x_s) \tag{4}$$

with x_s the starting position of damping zone and α (>0) an independent parameter which is adjusted to completely absorb the wave, avoiding wave reflection. Note that at $x=x_s$ $d(x)$ is zero (minimum value) and at the end of the tank $d(x)$ reaches the maximum value $\alpha(x_e-x_s)$ where x_e is the end position of damping zone.

The method of Volume of Fluids (VoF) offered by OpenFOAM is applied to capture wave surface. The VoF transport equation is

$$\frac{\partial F}{\partial t}+\frac{\partial(Fu)}{\partial x}+\frac{\partial(Fw)}{\partial z}=0 \tag{5}$$

where F is the fraction function and represents that a computational cell with $F=0$ is full of air, while if $F=1$ it is full of water and when $0<F<1$ the cell locates at the interface between water and air.

In present case, the initial condition considered at $t=0$ is a still water with no waves. The boundary conditions are as follows when solving the transport equations:

- For the piston boundary, a moving wall condition is set.
- At water bottom and the end side of the tank, a fixed wall condition is imposed on.
- At the atmosphere, a pressure-outlet condition is considered.

3. NUMERICAL METHOD

The present contributions to OpenFOAM lie in two aspects: implement a dynamic boundary condition and extend a solver by adding the damping term into the original one. The original solver extended here is named interDyMFoam. This solver is based on a finite volume method and can be used to simulate turbulence, while if the simulation type is turned to laminar mode the code is exactly to solve the equations (1), (2) and (3) without modelling turbulence. The damping term in equation (3) is added on the right side of the original momentum equation by defining a field variable. A class or dynamic boundary condition which inherits the old one "fixedValuePointPatchField" is developed to realize the movement of a boundary. The new class incudes a function being able to read data from a file, thus in the process of simulating the value imposed on the boundary can vary over time. In this study, the time history of the piston displacement is stored in a file beforehand and the displacement is updated in each time step according to the stored data when simulating wave generations.

OpenFOAM supplies a range of discretization schemes for the terms of time, convection and diffusion respectively and the solvers for system of linear equations as well. Here a second-order Central Difference Scheme (CDS) is chosen

©2017: The Royal Institution of Naval Architects

for the diffusive terms. The convective terms are discretized by a second-order Upwind Difference Scheme (UDS). For time, the first-order Euler scheme is employed. The systems of linear equations resulting from the discretized equations are solved by using iterative solvers, here Gauss-Seidel relaxation for velocity and Generalized Geometric Multi-Grid (GAMG) for pressure.

4. GENERATION OF FINITE-AMPLITUDE WAVES

4.1 MADSEN'S SECOND-ORDER WAVE-MAKER THEORY

According to Madsen's theory (Madsen, 1971), when the displacement of a piston is prescribed as

$$\xi = -\xi_0 \cos(\omega t) \tag{6}$$

the generated wave profile will be

$$\begin{aligned}\eta = \eta^{(1)} + \eta_p^{(2)} + \eta_l^{(2)} \\ = -a\sin(k_0 x - \omega t) - a_p^{(2)}\cos 2(k_0 x - \omega t) \\ + \cos(kx - 2\omega t)\end{aligned} \tag{7}$$

where

$$a = \frac{\xi_0 \tanh(k_0 h)}{n_1}, \tag{8}$$

$$a_p^{(2)} = \frac{k_0 a^2}{4}\frac{(2+\cosh(2k_0 h))\cosh(k_0 h)}{\sinh^3(k_0 h)} \tag{9}$$

and

$$\begin{aligned}a_l^{(2)} = \frac{a^2}{2}\frac{\coth(k_0 h)}{h}\left(\frac{3}{4\sinh^2(k_0 h)}\right. \\ \left. - \frac{n_1}{2}\right)\frac{\tanh(kh)}{n_2}\end{aligned} \tag{10}$$

with

$$n_1 = \frac{1}{2}\left(1 + \frac{2k_0 h}{\sinh(2k_0 h)}\right), \tag{11}$$

$$n_2 = \frac{1}{2}\left(1 + \frac{2kh}{\sinh(2kh)}\right). \tag{12}$$

The dispersion relationships are as follows.

$$\omega^2 = k_0 g \tanh(k_0 h), \tag{13}$$

$$4\omega^2 = kg\tanh(kh) \tag{14}$$

In above equations, ξ_0 is the magnitude of piston displacement, ω is frequency, a is the height of first-order wave, $a_p^{(2)}$ and $a_l^{(2)}$ are the second-order wave heights and k_0, k are wave numbers. The superscripts $^{(2)}$ refer to the order of magnitude of the terms.

The solution of wave profile, i.e., equation (7), is derived from potential theory. The first term on the right-hand side represents the first-order wave component. The second term is the Stokes second-order wave which travels at the same speed as the first-order one. The third term is the free wave of second order with a lower speed than the speed of the first-order wave, which consequently results in that the wave profile is not of permanent form.

The second harmonic free wave can be eliminated by adding a second-order piston motion. If the resultant displacement of piston is then give by

$$\begin{aligned}\xi = -\xi_0\left\{\cos(\omega t)\right. \\ + \frac{1}{2}\frac{a}{h}\frac{1}{n_1}\left(\frac{3}{4\sinh^2(k_0 h)}\right. \\ \left.\left. - \frac{n_1}{2}\right)\sin(2\omega t)\right\}\end{aligned} \tag{15}$$

the generated wave is Stokes second-order wave with a permanent form. The solution of surface elevation is

$$\begin{aligned}\eta = a\cos(k_0 x - \omega t) \\ + \frac{\pi}{2}\frac{a^2}{\lambda}\frac{\cosh(k_0 h)}{\sinh^3(k_0 h)}(2 \\ + \cosh(2k_0 h))\cos 2(k_0 x - \omega t)\end{aligned} \tag{16}$$

where λ is wave length.

4.2 SIMULATION OF WAVE MAKER

Madsen did some experiments to verify his theory, which offered a good source for present validation. In this study, the piston motions prescribed by both equations (6) and (15) are considered. According to the experiments by Madsen, for present simulations a virtual 2-D wave tank is set up with the long of 50 meters and 0.76-meter height, where the water depth is 0.38 meter. The zone of the virtual tank $30\,m \le x \le 50\,m$ is imposed for wave absorption and for all simulations the damping parameter α in equation (4) is specified to 3 which can ensure an absolute absorption of wave based on a few pre-computations. Since the temperature or properties of water and air was not mentioned by Madsen in his experiment, the density and viscosity coefficient of water and air are set to the values at $20°C$ in the simulations. The temperature is usually expected to have ignorable impacts on the general conclusions.

©2017: The Royal Institution of Naval Architects

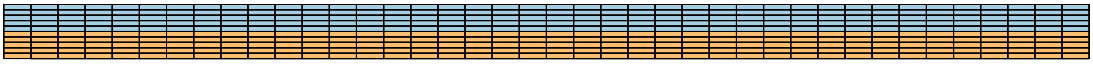

Figure 2 A structured grid

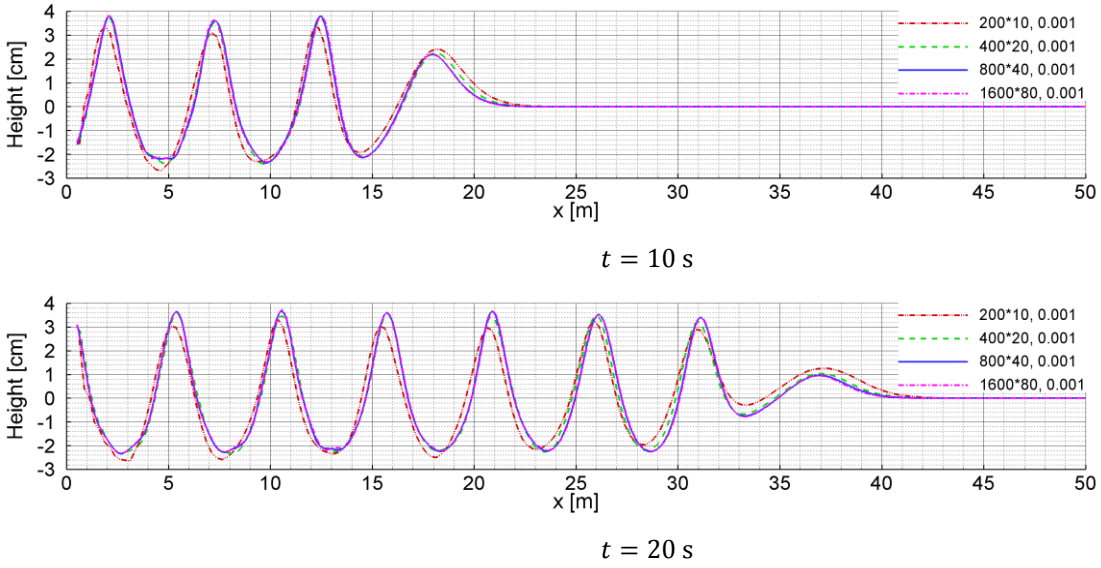

Figure 3 Computed wave profiles from the grid dependency study

Structured grids are generated for the simulations by using the mesh tool "blockMesh" included in OpenFOAM. The computational domain is divided equally in x and z directions respectively, i.e., the edge length of cell is same in each direction. Figure. 2 shows an example of a very coarse grid (just a partial view), for which the water and air are labelled with different colours (the orange is water) in still water.

4.2.1 Grid dependency study

The sensitivities of wave profile to grid density and time step are firstly investigated for the piston motion given by equation (15). Four grids are generated by systematically doubling the number of grid points in x and z directions. Table 1 lists the gird information. The cell number increases with the growth rate of 4 times. The case $\xi_0 = 6.1$ cm and $T = 2.75$ s is taken, consistent with Madsen's experimental condition, where T is wave period and equal to $2\pi/\omega$. The computational time step Δt is same for all grids and set to be 0.001 s.

Table 1 Grid information

Grid	Dimensions
Coarse	200×10
Medium	400×20
Fine	800×40
Finer	1600×80

Figure 3 presents the computed wave profiles at $t = 10$ s and $t = 20$ s. The wave has not yet propagated to the end of the tank at $t = 20$ s. We note from the figure that when refining the grid, the difference of profile becomes smaller gradually and the profiles based on the fine and finer grids are nearly identical. An evident phase lag is observed for the profile from the coarse grid compared with the profiles based on other grids. A more non-linear characteristic of the wave trough is found at a close distance from the piton, e.g., in the range of 0 to 15 meters. Generally, a finer grid captures better the characteristic. It seems that the density of the fine grid is enough for highly accurate results via the comparison.

4.2.2 Time-step dependency study

Time-step dependency study is carried out for the same case, i.e., $\xi_0 = 6.1$ cm, $T = 2.75$ s and displacement by equation (15), using the above gird with dimensions 800×40. Another three time steps of 0.002 s, 0.005 s and 0.025 s are further considered. The computed wave profiles at $t = 10$ s and $t = 20$ s are shown in Figure 4. The largest difference among the profiles is displayed by the wave amplitude. As reducing the time step, the change of wave amplitude becomes smaller. The wave phases are same. For $\Delta t = 0.025\ s$, the wave decays more quickly than others. At small time steps, the wave trough also shows a non-linear characteristic in the range of 0 to 15 meters, while when Δt is equal to $0.025\ s$ the characteristic vanishes.

©2017: The Royal Institution of Naval Architects

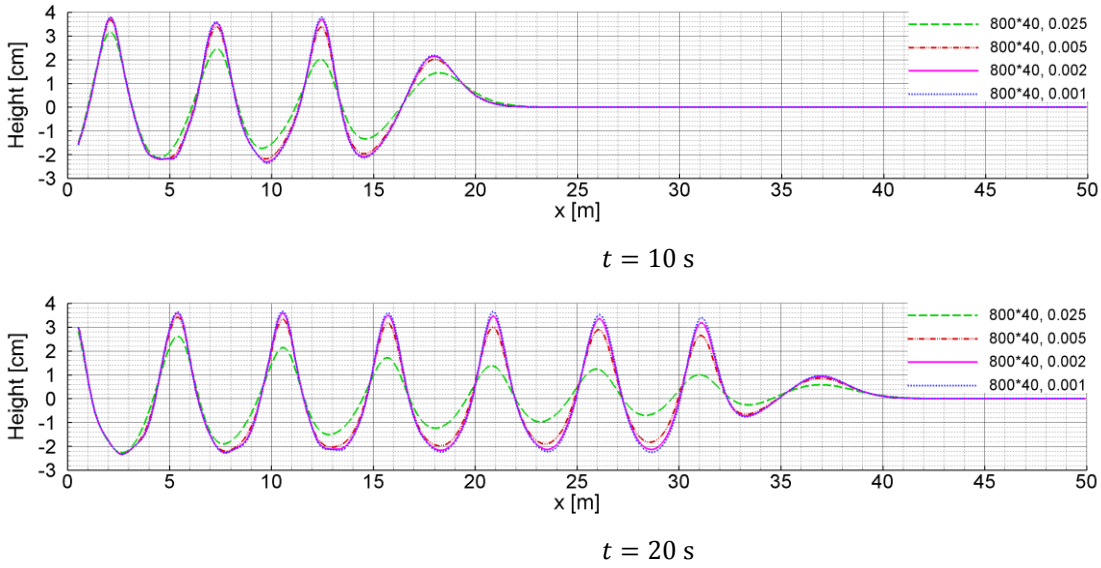

Figure 4 Computed wave profiles from the time-step dependency study

4.2.3 Comparison with measured data and analytical solution

Figure 5 shows comparisons of the numerical wave profiles at $x = 4.9$ m and $x = 8.7$ m with measured data and analytical solution determined by equation (16). We note that both computed results and analytical solution are consistent to those recorded in laboratory. Satisfactory agreements are also observed in Figure. 6 for the other case with $\xi_0 = 6.1$ cm, $T = 2.75$ s and piston displacement prescribed by equation (6). In this case, the profiles at the stations $x = 4.9$ m and $x = 8.7$ m are more largely different, shown by simulations, experiment and analytical solution as well. This is quite understandable since the profile includes the component of second-order free wave whose speed is lower than the main first-order wave, thus the resulting wave is not of permanent form as stated previously. In contrast, the distinction of profiles shown in Figure. 5 at $x = 4.9$ m and $x = 8.7$ m are not so large, because the free wave has been eliminated by the added second-order displacement in equation (6). On the whole, we can conclude via the comparisons that the present simulations succeed in generating the second-order waves. The computed wave profiles are of certain accuracy.

It should be noted that the wave profiles based on experiments were obtained from a 3D wave tank with 46 cm width. The width might be enough to get the accuracy profiles of 2D waves, i.e., the effects of side walls could be ignored.

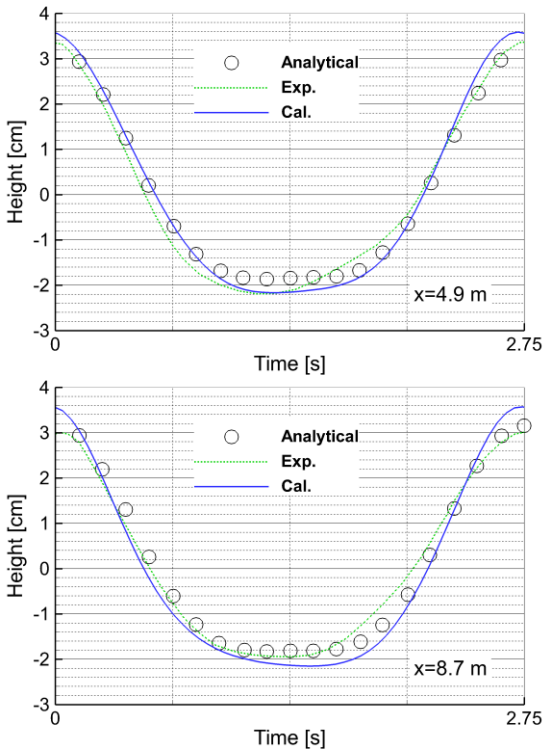

Figure 5 Comparison of the predicted wave height at two stations in one period with measured data and analytical solution for the case $\xi_0 = 6.1$ cm, $T = 2.75$ s and piston displacement given by equation (15)

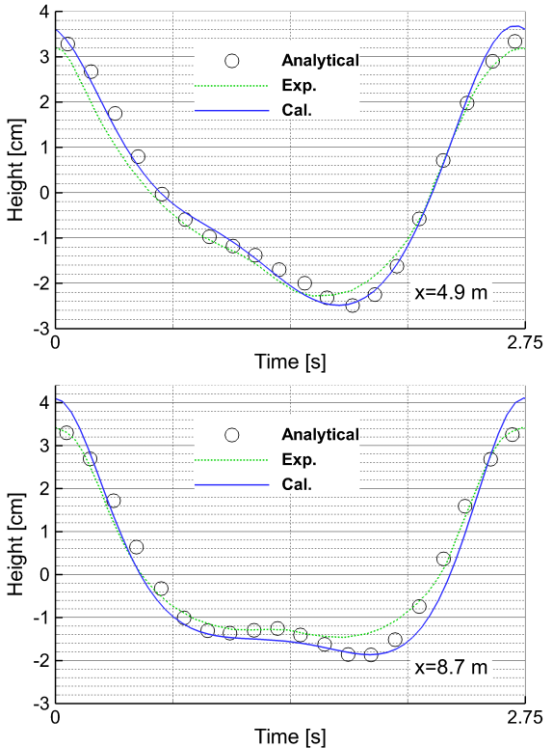

Figure 6 Comparison of the predicted wave height at two stations in one period with measured data and analytical solution for the case $\xi_0 = 6.1$ cm, $T = 2.75$ s and piston displacement given by equation (6)

In order to clarify the effects of the harmonic free wave on the wave surface, Figure. 7 compares the computed wave profiles obtained by prescribing the piston displacements by equations (6) and (15). The comparisons are at $t = 10$ s and $t = 20$ s respectively. It is shown that the difference between the profiles depends on the distance from the piston. At a position closer to the piston, the difference is larger, whereas at a further distance the difference becomes smaller. This phenomenon may be explained by that the harmonic free wave travels more slowly than other wave components, and therefore the free wave does not yet propagate to a far distance.

5. CONCLUSIONS

This work has presented a study on generating waves using the own developed code based on OpenFOAM. First of all, the theoretical backgrounds are described. Then the Madsen's second-order waves in a 2D virtual tank were simulated. Convergence study showed that the 'fine mesh' with time interval of 0.001 s was satisfactory in the calculations. The computed results were discussed and validated by comparisons with measured data and analytical solutions. A good match was achieved for the considered case. However, the present solver is only applied for generating long finite-amplitude waves. A wide range of validation can be further done for more practical cases, e.g., wave steepness for which viscous effect will be obvious.

The present work is of great practical significance. Generally speaking, the desired wave with a permanent form in two or three dimensions can be generated numerically by using the present solver with the relevant input of the piston displacement, which can be applied for the study on the dynamic response of marine structures in waves, for example ship seakeeping performance. In future work, the researches on the wave and structure interaction are going to be focused on.

6. ACKNOWLEDGEMENT

This work was supported by National Natural Science Foundation of China (Grant No. 51609188, 51609187, 51609186), Hubei Key Laboratory of Inland Shipping Technology (Grant No. NHHY2015002) and Fundamental Research Funds for the Central Universities (WUT: 2016IVB006, 2017IVB007).

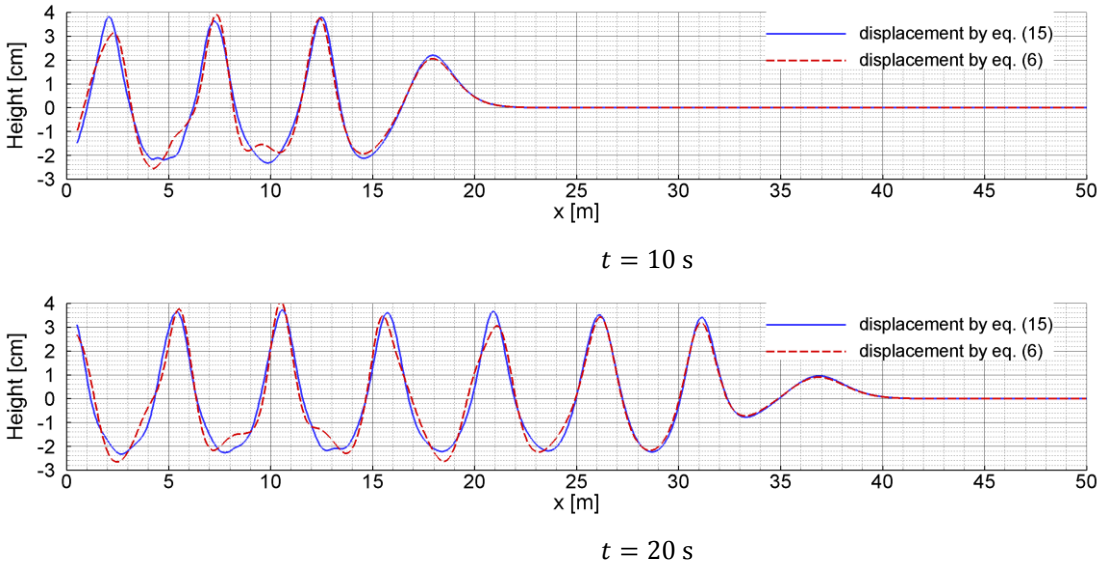

Figure 7 Comparisons between the computed profiles based on the piston displacements given by equations (6) and (15)

©2017: The Royal Institution of Naval Architects

7. REFERENCES

1. DONG, C. M. and HUANG C. J. (2001), *On a 2-D numerical wave tank in viscous fluid,* Proceedings of the eleventh international offshore and polar engineering conference, Stavanger, Norway, pp. 148-155.
2. GRILLI, S.T., GUYENNE, P. and DIAS, F. (2001), *A fully nonlinear model for three-dimensional overturning waves over arbitrary bottom,* International journal for numerical methods in fluids, 35(7), pp. 829-867.
3. HAFSIA, Z., HADJ, M. B., LAMLOUMI, H. and MAALEL, K. (2009), *Internal inlet for wave generation and absorption treatment, Coastal engineering,* 56, pp. 951-959.
4. HAVELOCK, T. H. (1929), *Forced surface wave on water,* Philosophical Magazine, Series 7, Vol. 8, pp. 569-576.
5. MADSEN, O. S. (1971), *On the generation of long waves,* Journal of geophysical research, 76(36), pp. 8672-8683.
6. SCHÄFFER, H. A. (1994), *Second-order wave-maker theory for irregular waves*, Ocean engineering, (23)1, pp. 47-88.
7. SULISZ, W. and PAPROTA, M. (2008), *Generation and propagation of transient nonlinear waves in a wave flume,* Coastal engineering, 55, pp. 277-287.
8. URSELL, F., DEAN, R. G. and YU, Y. S. (1960), *Force small-amplitude water waves: a comparison of theory and experiment*, Journal of fluid mechanics, Vol. 7, pp. 32-53.
9. ZHANG, H. and SCHÄFFER, H. A. (2007), *Approximate stream function wave-maker theory for highly non-linear waves in wave flumes*, Ocean engineering, 34, pp. 1290-1302.

©2017: The Royal Institution of Naval Architects